Electronic Supplementary Material (ESI) for Journal of Materials Chemistry C.
This journal is © The Royal Society of Chemistry 2014

Molecular weight sensing properties of ionic liquid-polymer composite films: theory and experiment

Bishnu P. Regmi,[a] Nicholas C. Speller,[a] Michael J. Anderson,[b] Jean Olivier Brutus,[c] Yonathan Merid,[a] Susmita Das,[a] Bilal El-Zahab,[d] Daniel J. Hayes,[e] Kermit K. Murray,[a] and Isiah M. Warner*[a]

[a]Department of Chemistry, Louisiana State University, Baton Rouge, LA 70803, USA.
[b]Department of Chemistry, Columbus State University, Columbus, GA 31907, USA
[c]Biomedical Engineering Department, State University of New York at Stony Brook, Stony Brook, NY 11790, USA
[d]Mechanical and Materials Engineering Department, College of Engineering and Computing, Florida International University, Miami, FL 33174, USA
[e]Department of Biological and Agricultural Engineering, Louisiana State University, Baton Rouge, LA 70803, USA.
*Corresponding author: Tel: +1225-578-2829. Fax: +1 225-578-3971. E-mail: iwarner@lsu.edu

SUPPORTING INFORMATION

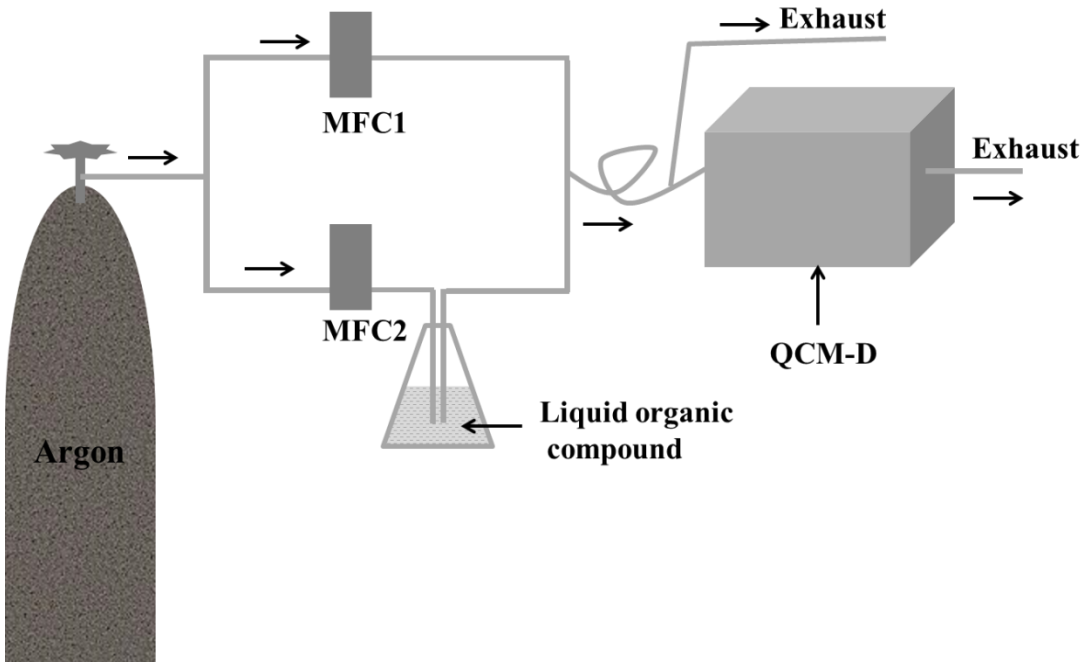

Fig. S1 Schematic of experimental setup used for vapor generation and measurement.

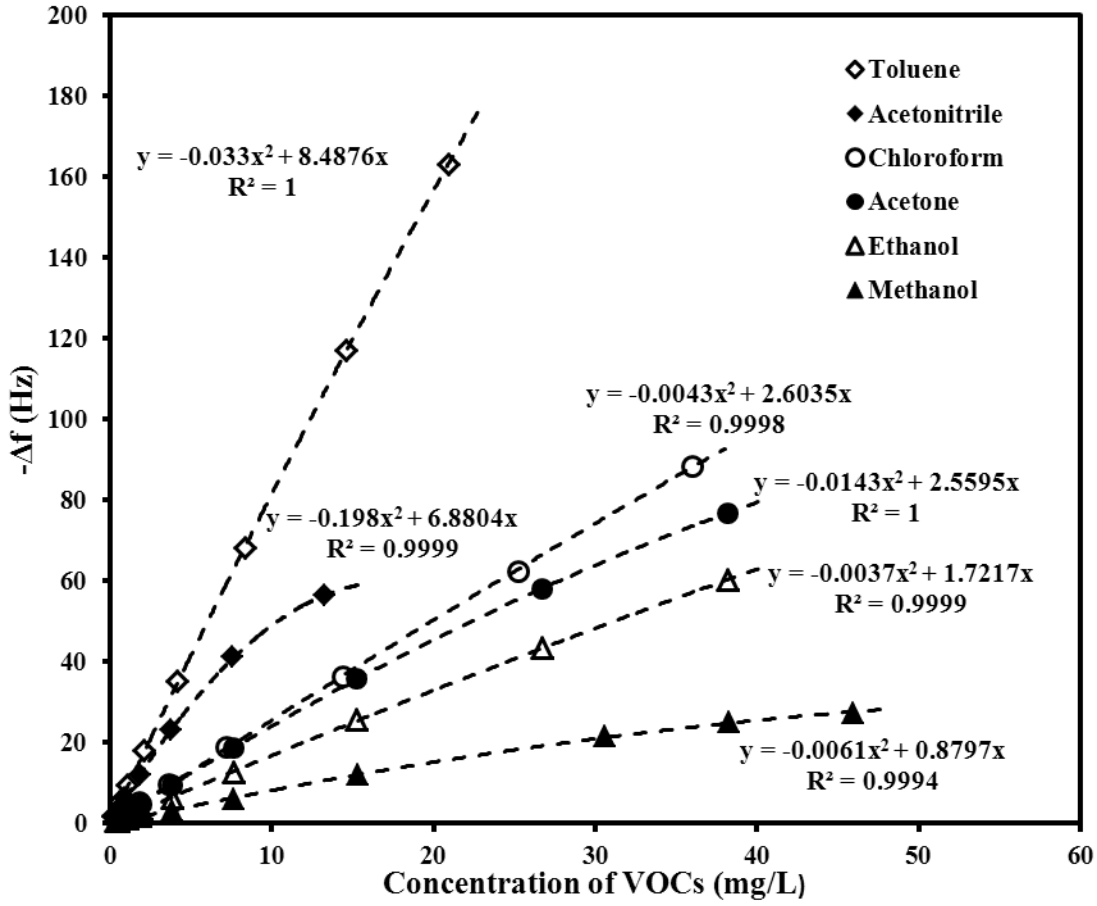

Fig. S2 Plots showing the variation of Δ*f* with concentration of VOCs for a QCM sensor coated with [HMPyr][PF_6]. Amount of coating material: 83 μg.cm^{-2}. Each analyte exhibits a second-degree polynomial relationship between Δ*f* and concentration.

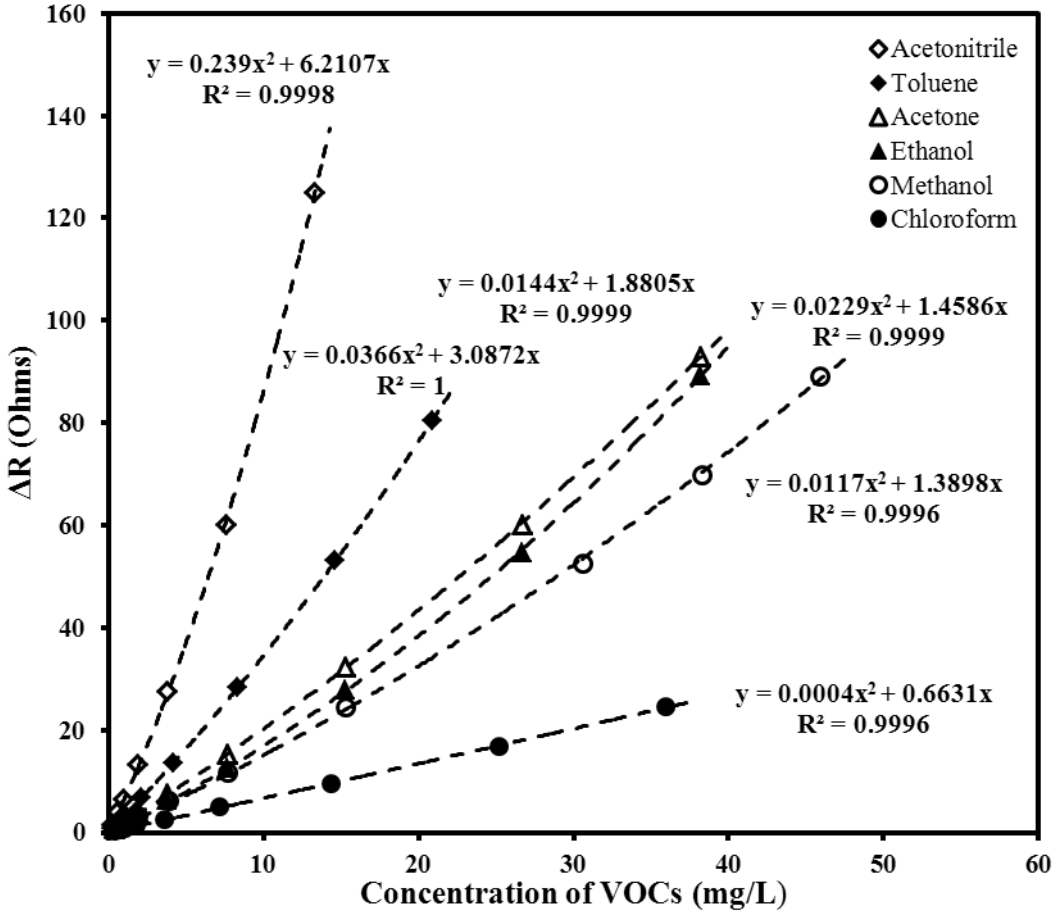

Fig. S3 Plots showing the variation of Δ*R* with concentration of VOCs for the same sensor shown in Figure S2. Each analyte is showing a second-degree polynomial relationship between Δ*R* and concentration.

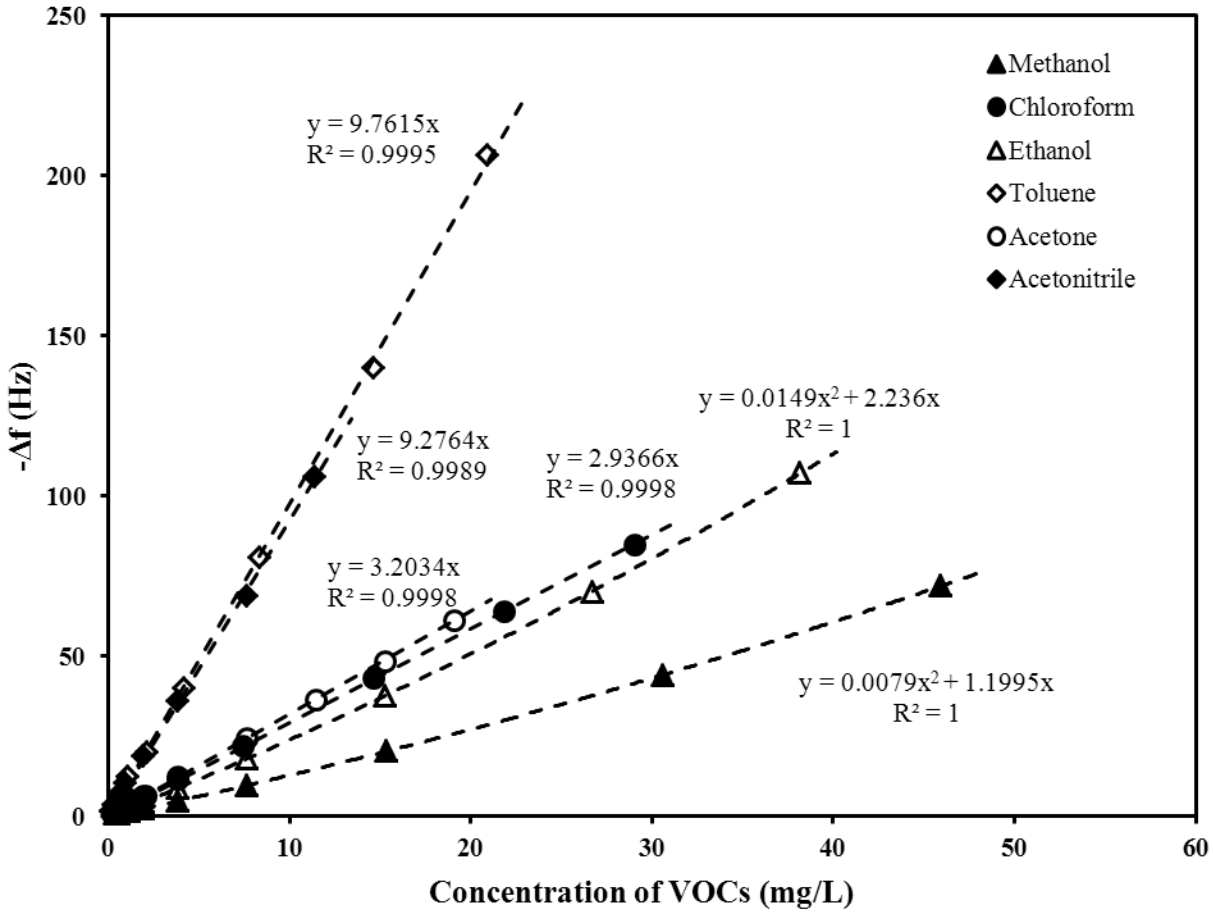

Fig. S4 Plots showing the magnitude of frequency shift of a QCM sensor coated with [HMPyr][PF_6]-PMMA on exposure to varying concentration of organic vapor. Amount of sensing material: 90 µg.cm^{-2}. Methanol and ethanol are slightly more polynomial, while others are linear.

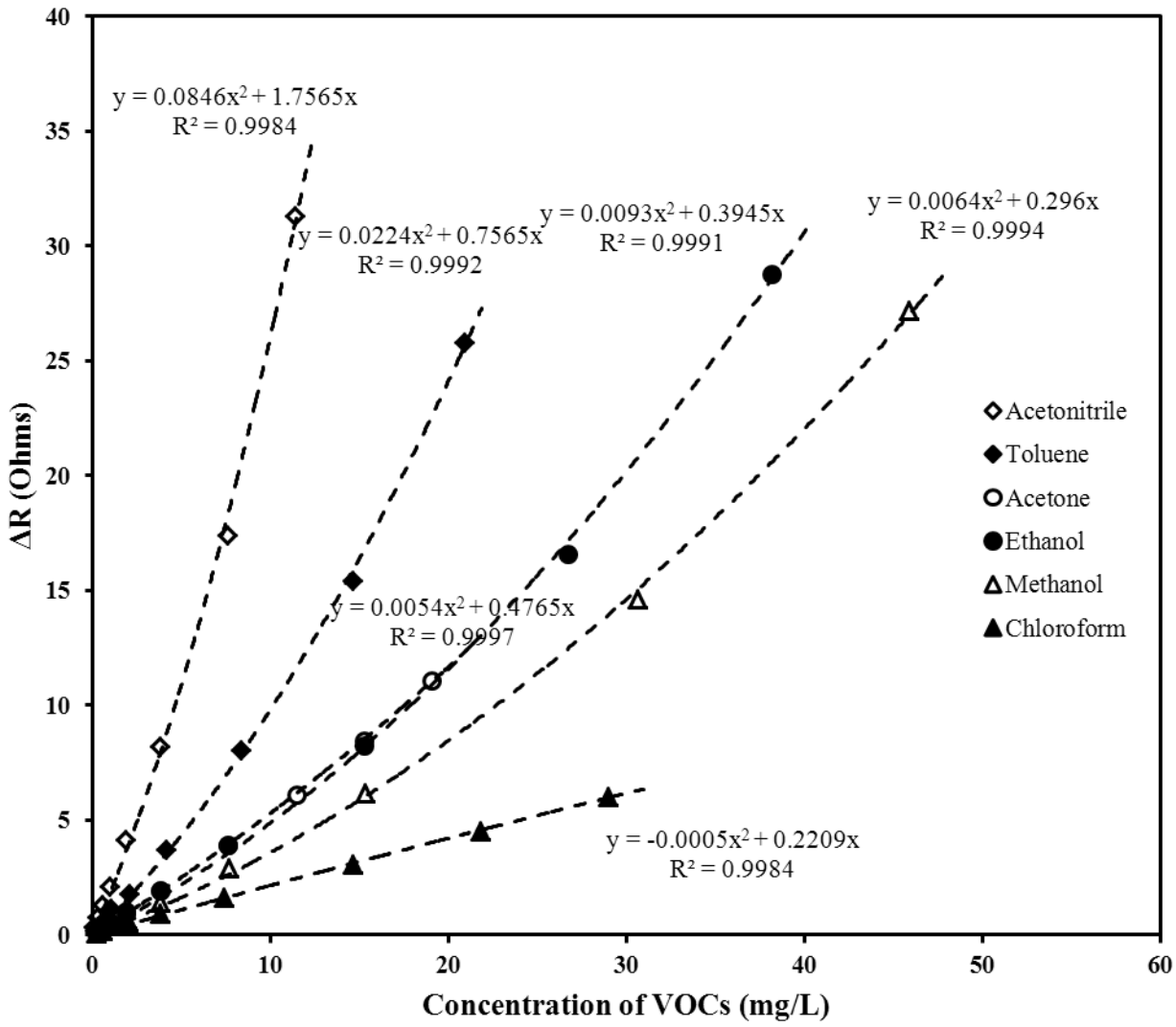

Fig. S5 Plots showing the motional resistance shift of a QCM sensor coated with [HMPyr][PF_6]-PMMA on exposure to varying concentration of organic vapor. Amount of sensing material: 90 $\mu g.cm^{-2}$. Each analyte shows a second-order polynomial relationship between motional resistance shift and the vapor concentration.

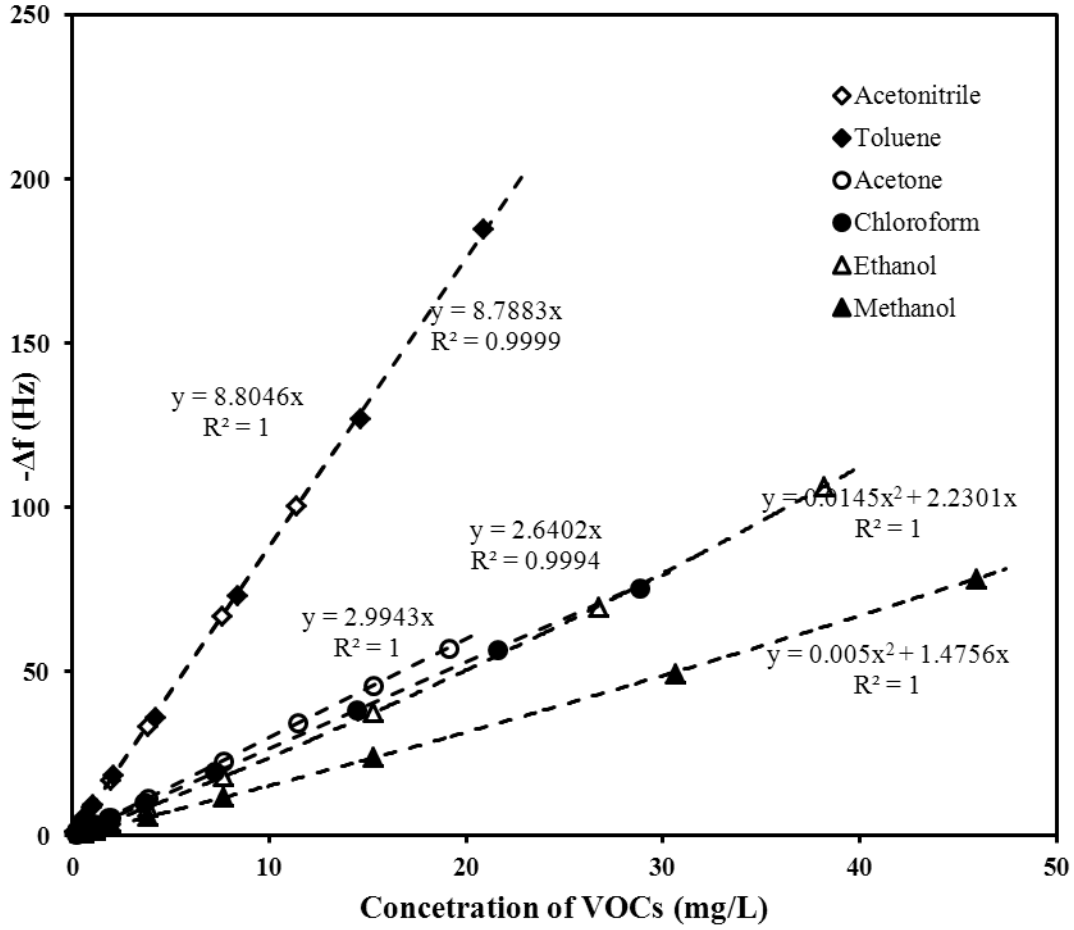

Fig. S6 Plots showing the magnitude of frequency shift of a QCM sensor coated with [HMPyr][PF_6]-CA on exposure to varying concentration of organic vapor. Amount of sensing material: 85 µg.cm^{-2}. Each analyte shows a second-order polynomial relationship between the frequency shift and the vapor concentration.

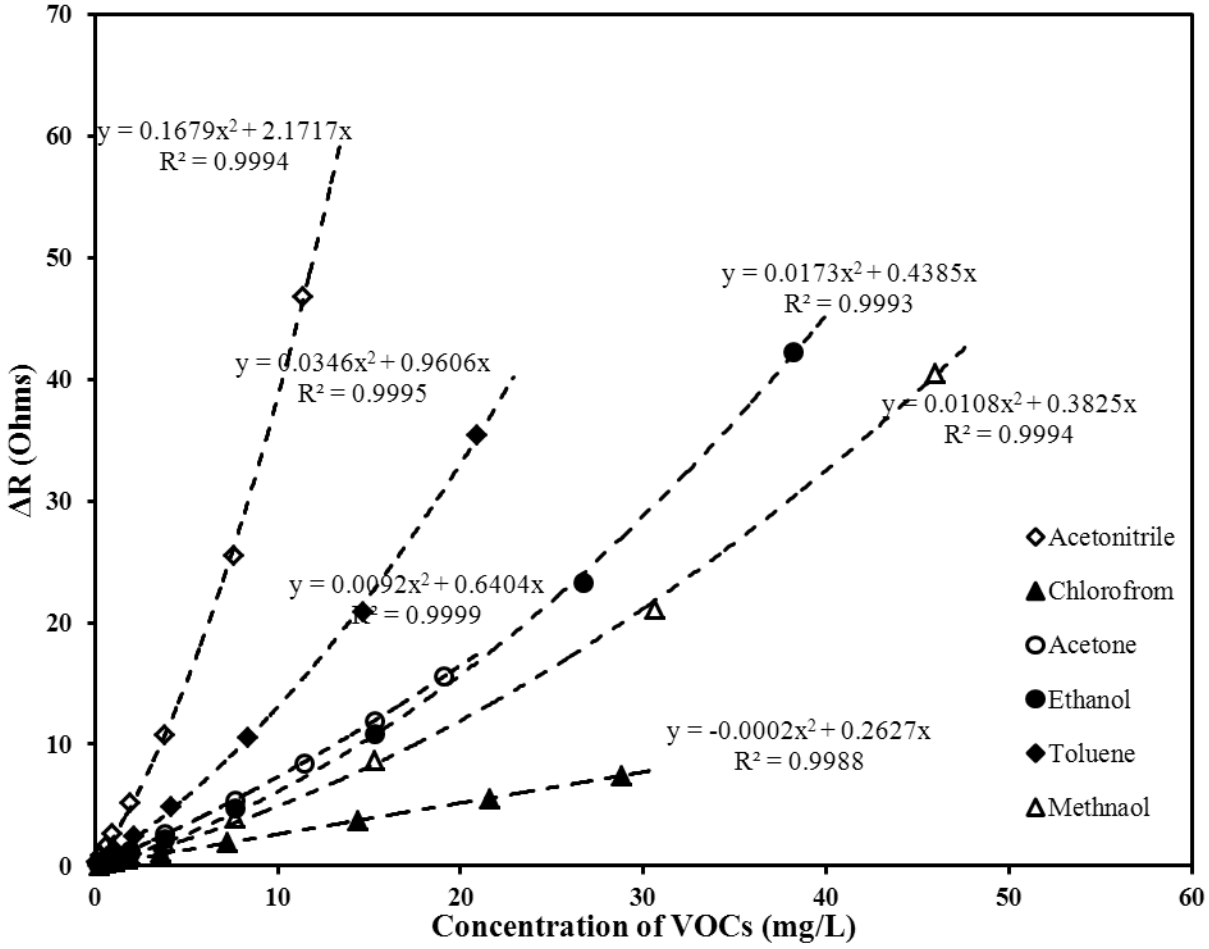

Fig. S7 Plots showing the frequency shift of a QCM sensor coated with [HMPyr][PF_6]-CA on exposure to varying concentration of organic vapor. Amount of sensing material: 85 µg.cm^{-2}.

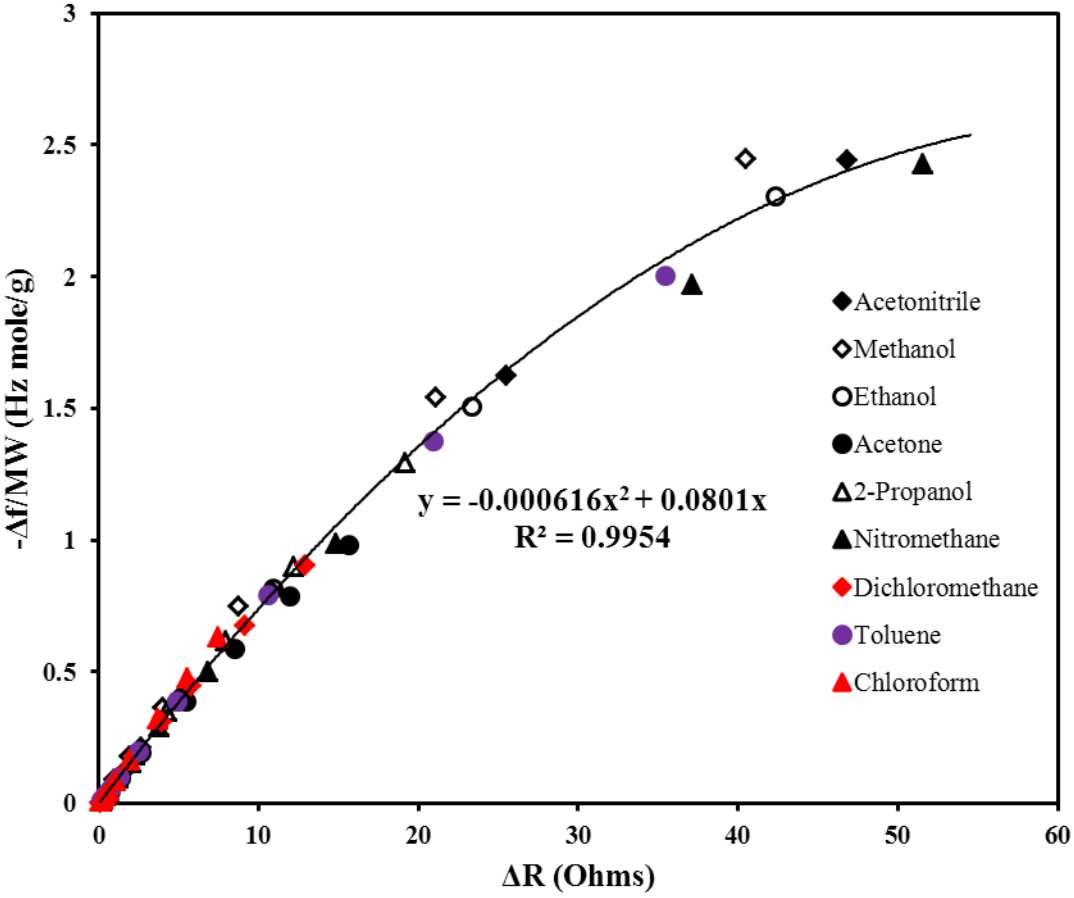

Fig. S8 Plot of the ratio of frequency shift to molecular weight against motional resistance shift of a QCM sensor coated with [HMPyr][PF_6]-CA for nine different organic vapors. Concentration ranges of the vapors are 0.574 to 45.9 mg.L^{-1} for methanol, 0.114 to 11.4 mg.L^{-1} for acetonitrile 0.382 to 38.2 mg.L^{-1} for ethanol, 0.191 to 19.1 mg.L^{-1} for acetone, 0.190 to 26.6 mg.L^{-1} for 2-propanol, 0.138 to 6.88 mg.L^{-1} for nitromethane, 0.321 to 64.2 mg.L^{-1} for dichloromethane, 0.125 to 20.9 mg.L^{-1} for toluene, and 0.216 to 29.0 mg.L^{-1} for chloroform.

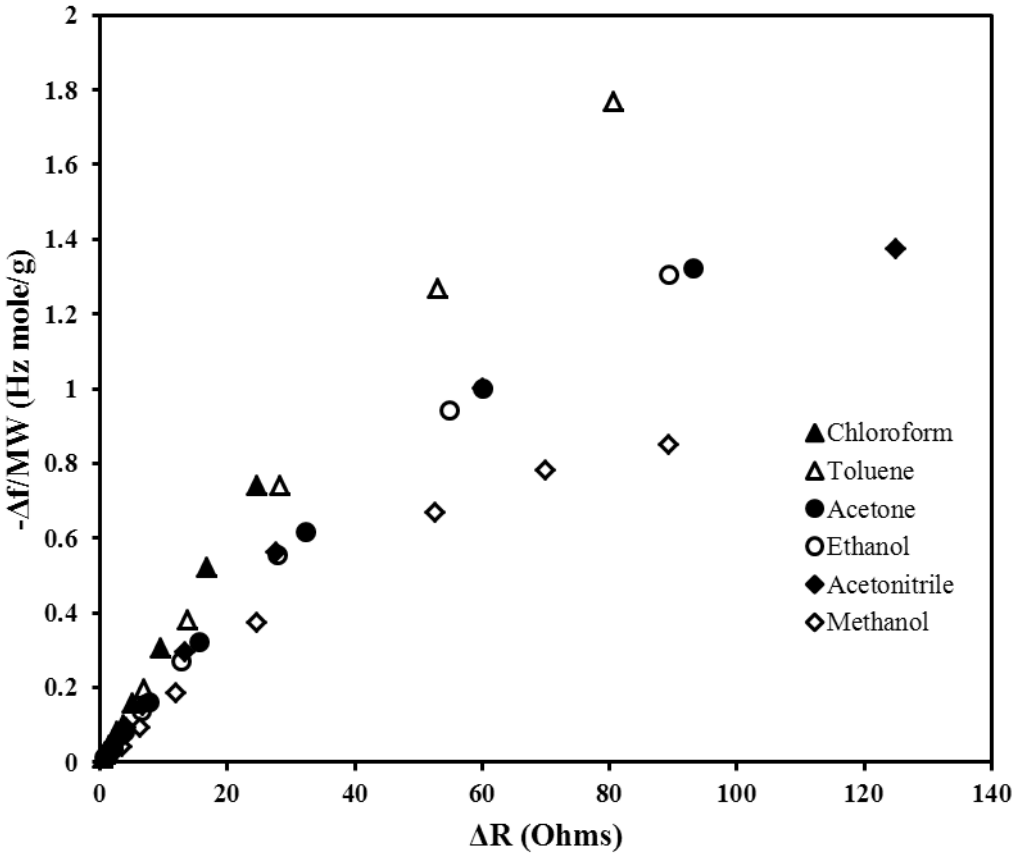

Fig. S9 Plot of the ratio of frequency shift to molecular weight against motional resistance shift of a QCM sensor coated with [HMPyr][PF_6]-only for six different organic vapors.

.

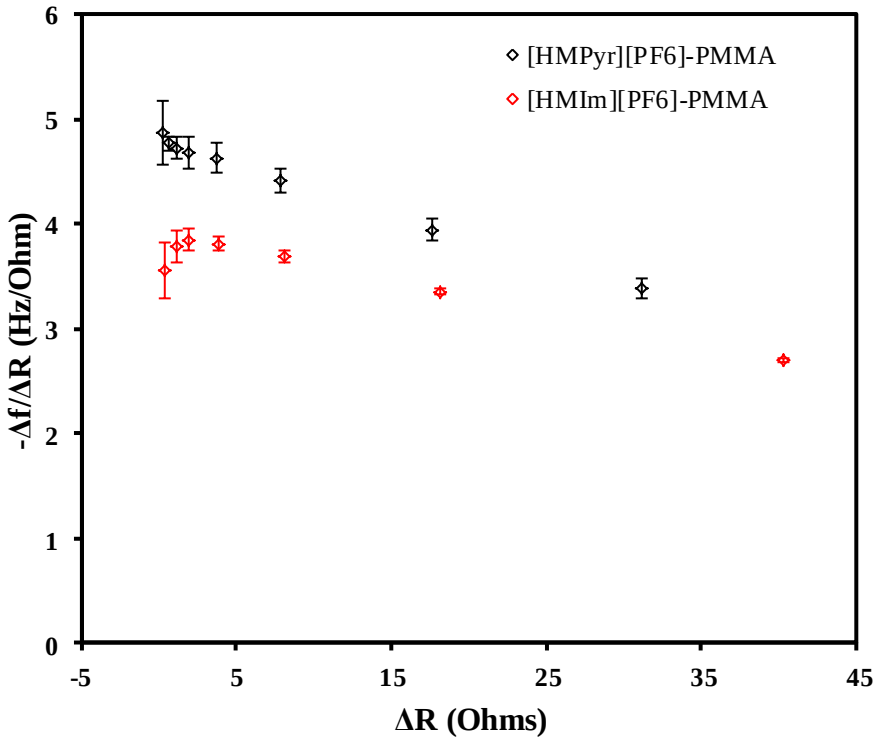

Fig. S10 Plot of $\frac{\Delta f}{\Delta R}$ versus ΔR (mean) for two different coatings during the absorption of acetonitrile vapors. Error bars represent the standard deviation of three replicate measurements. Except for the first point, for each coating, which lies near the detection limit, the relative standard deviation of other points lies between 1 to 4 percent. For [HMPyr][PF_6]-PMMA coated sensor each set of measurements were taken in an interval of three hours, while for [HMPIm][PF_6]-PMMA the measurements were taken in an interval of 1 hour. The larger standard deviations may be due to fluctuations in temperature.

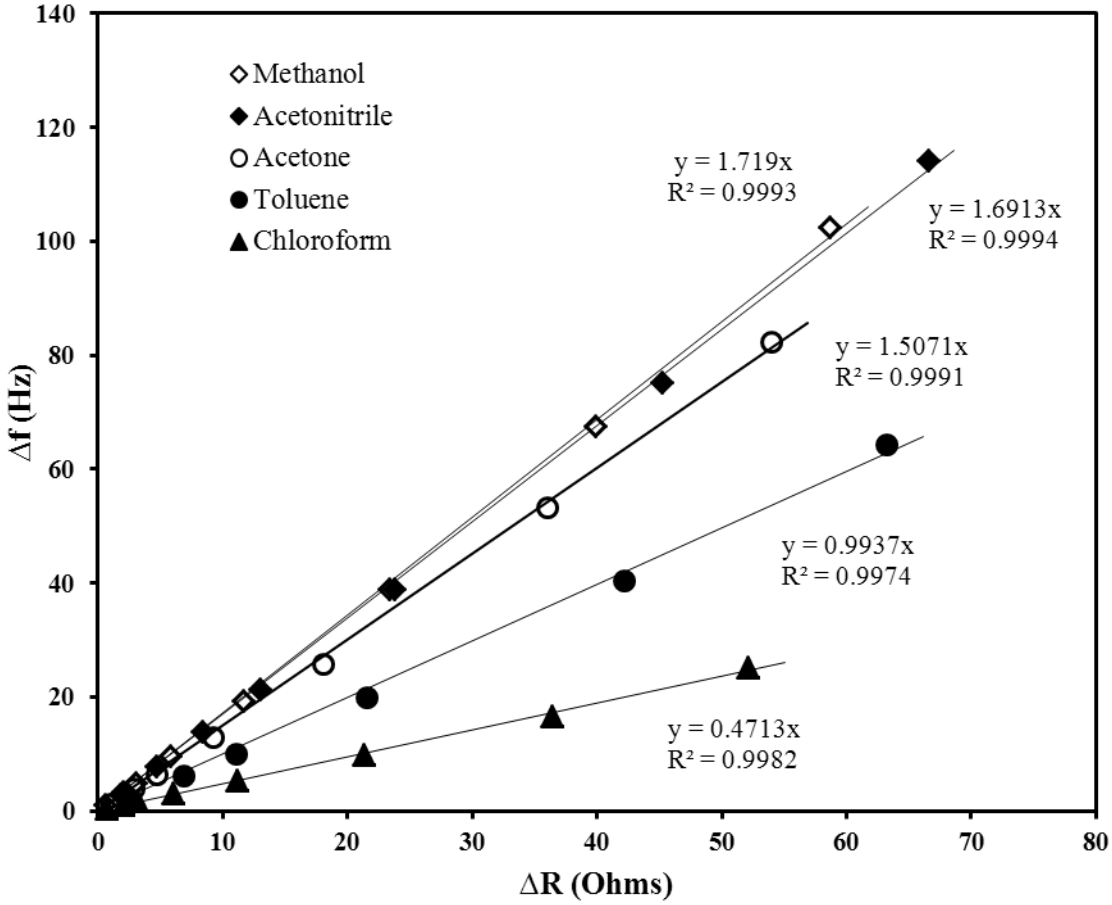

Fig. S11 Plots showing the variation of Δf with ΔR for a QCM sensor coated with [HMPyr][TFSI] upon exposure to five different organic vapors. Concentration ranges of the vapors are 0.191 to 19.1 mg L^{-1} for methanol, 0.114 to 5.70 mg L^{-1} for acetonitrile 0.191 to 11.4 mg L^{-1} for acetone, 0.210 to 6.27 mg L^{-1} for toluene, and 0.360 to 36.0 mg L^{-1} for chloroform.

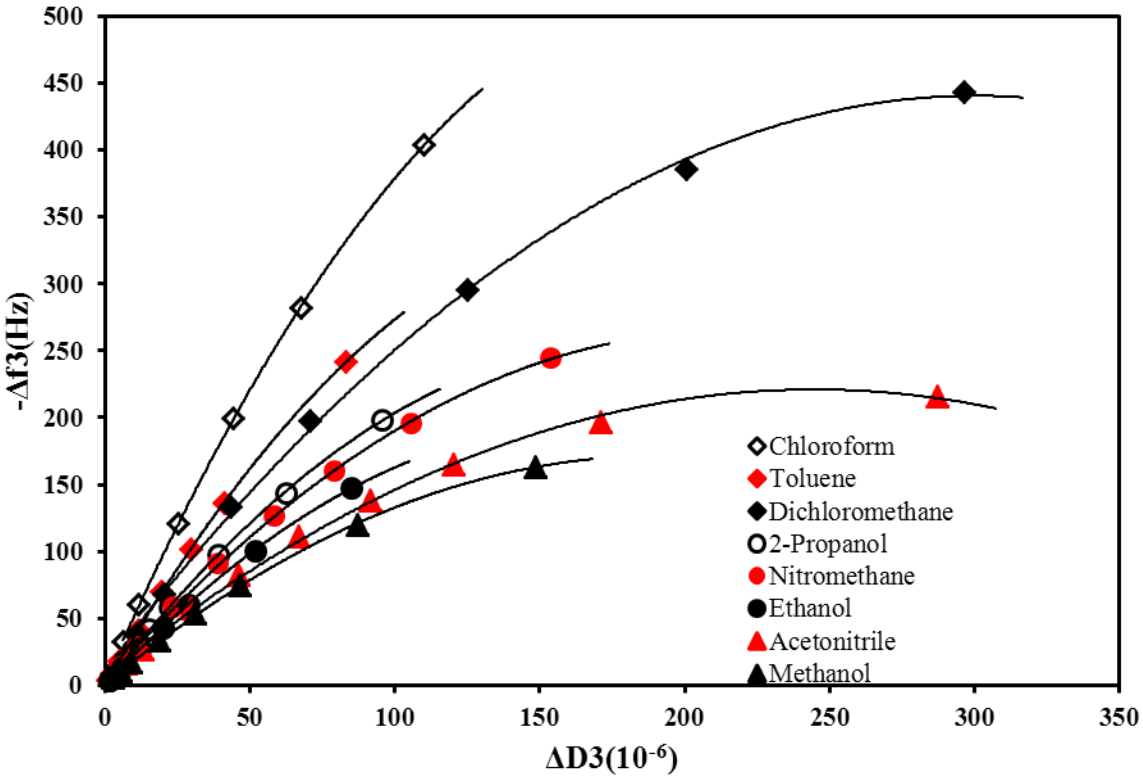

Fig. S12 Third harmonic Δ*f* versus Δ*D* plots for different analytes.

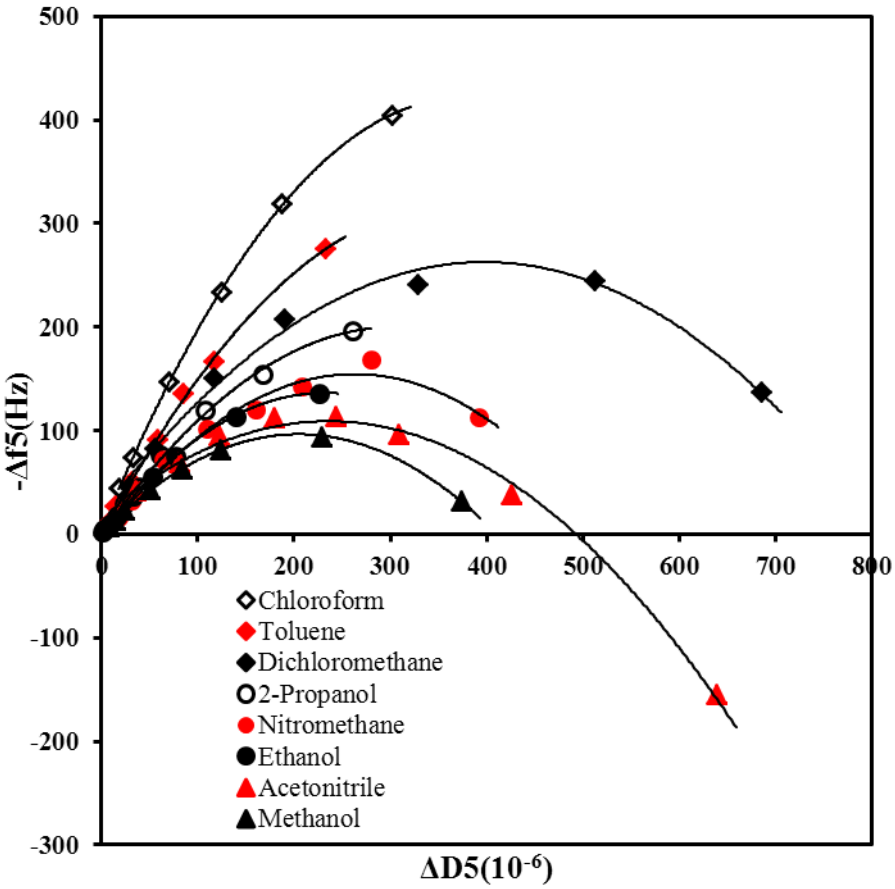

Fig. S13 Fifth harmonic Δ*f* versus Δ*D* plots for different analytes.

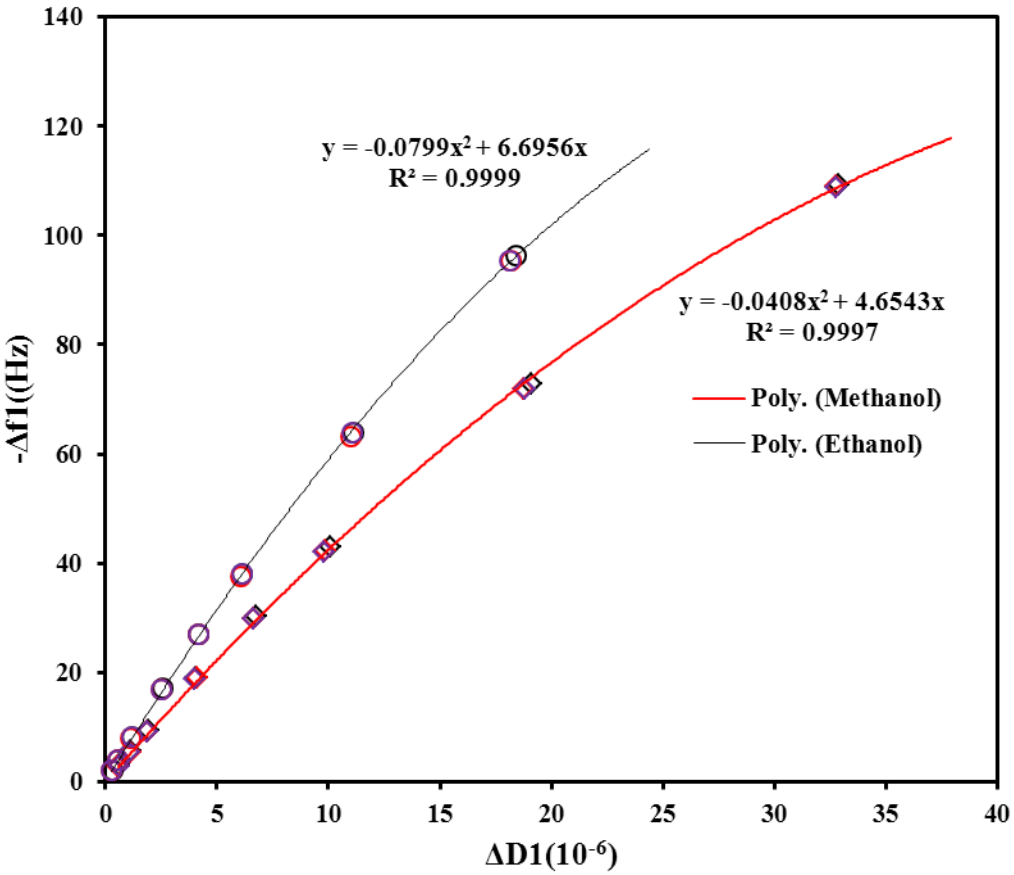

Fig. S14 Frequency shift versus dissipation shift plots for the first harmonic of a QCM-D coated with [HMPyr][PF_6]-PMMA during absorption of methanol and ethanol vapors. For each compound, three replicate measurements were performed in the concentration range of 1.5% to 40% of the saturated vapor concentration. The relative standard deviation of $\frac{\Delta f}{\Delta R}$ for each concentration tested was found to be between 0.1% and 1%.

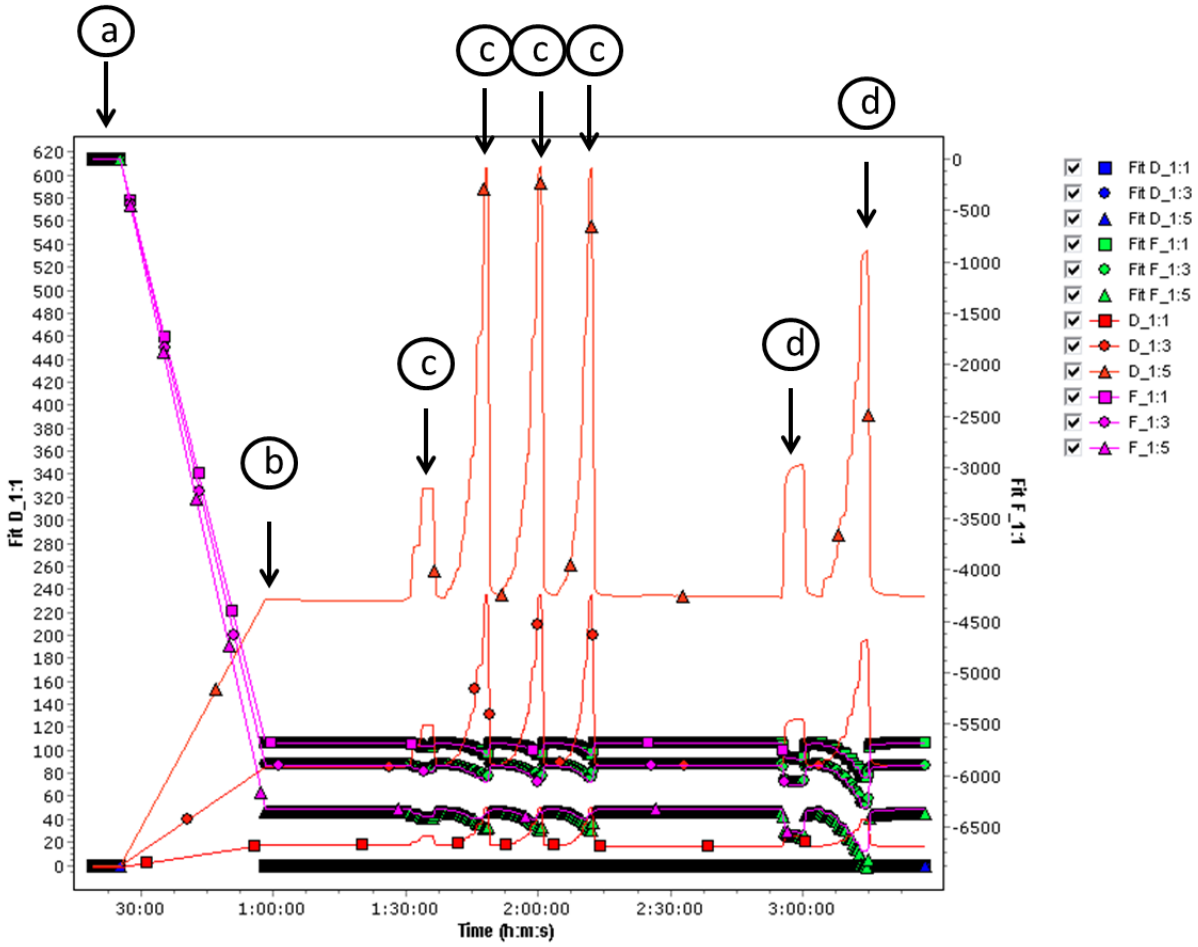

Fig. S15 Representative QCM-D data displaying experimental and fit values frequency and dissipation changes for the first, third, and fifth harmonics. The film was assumed to be purely elastic. Arrows represent: (a) bare quartz crystal, (b) after coating with [HMPyr][PF_6]-PMMA, (c) during exposure to methanol vapors, and (d) during exposure to chloroform vapors.

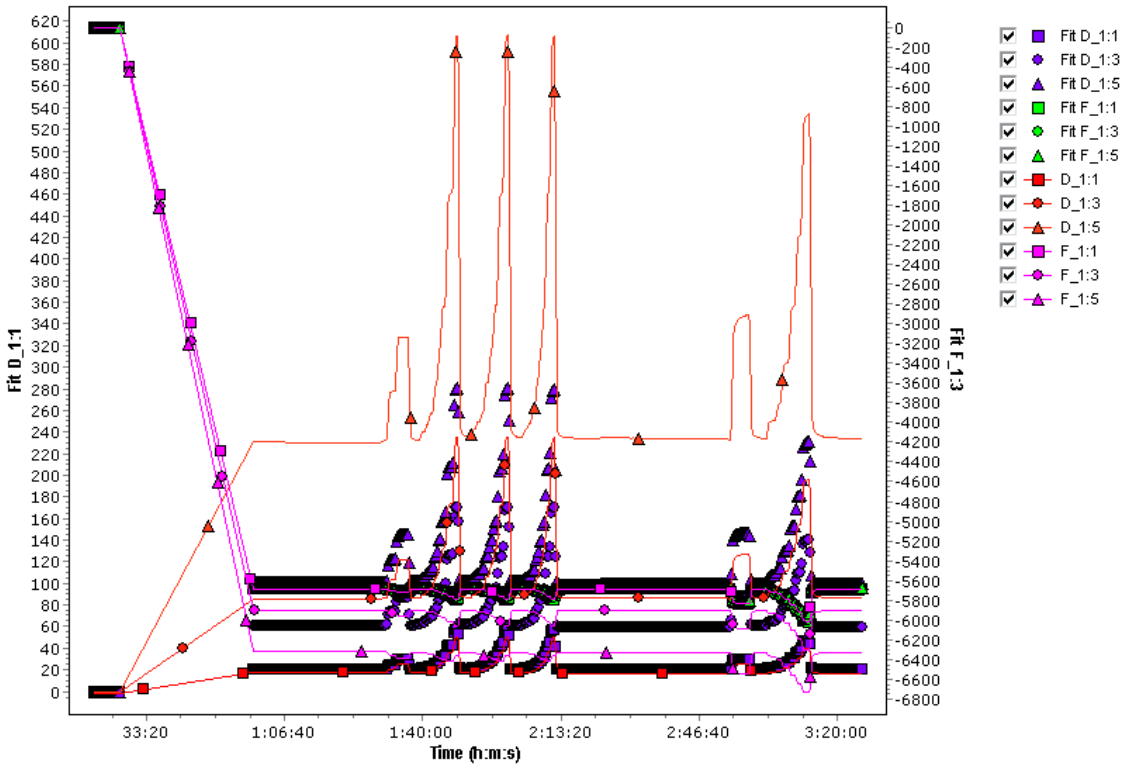

Fig. S16 The experimental and fit values of Δf and ΔD by assuming the film to be purely viscous.

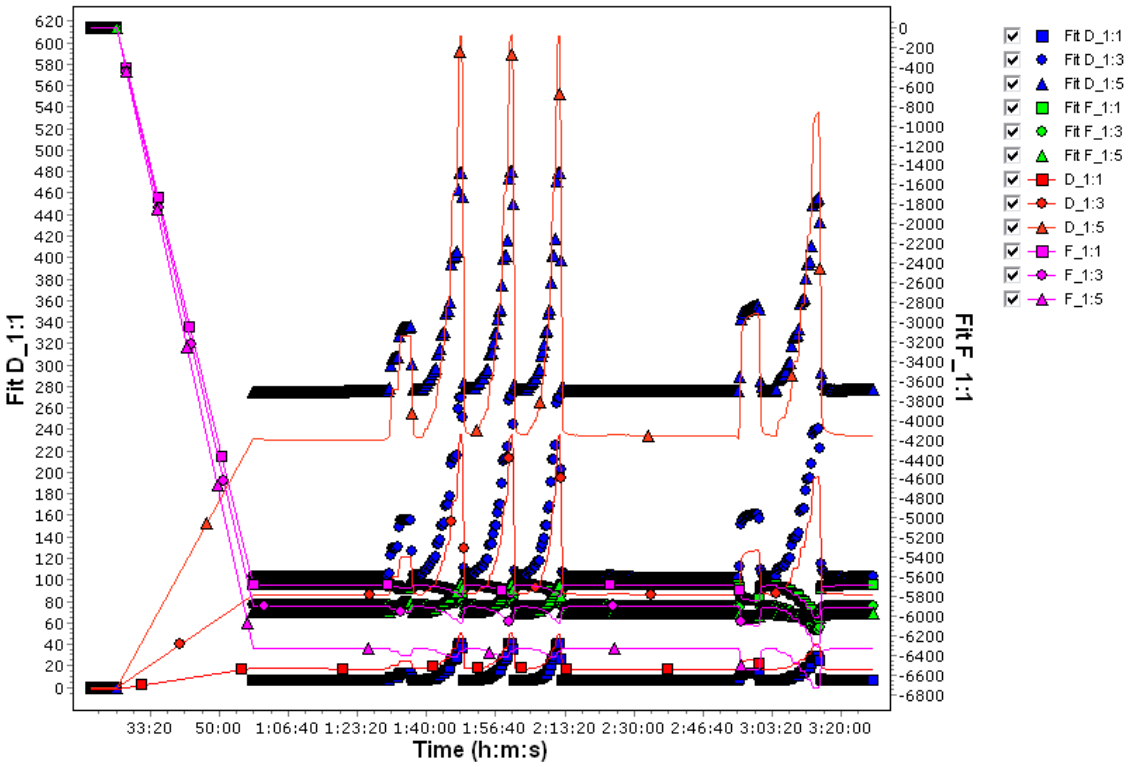

Fig. S17 The experimental and fit values of Δf and ΔD by assuming the film follows the Voigt viscoelastic model.

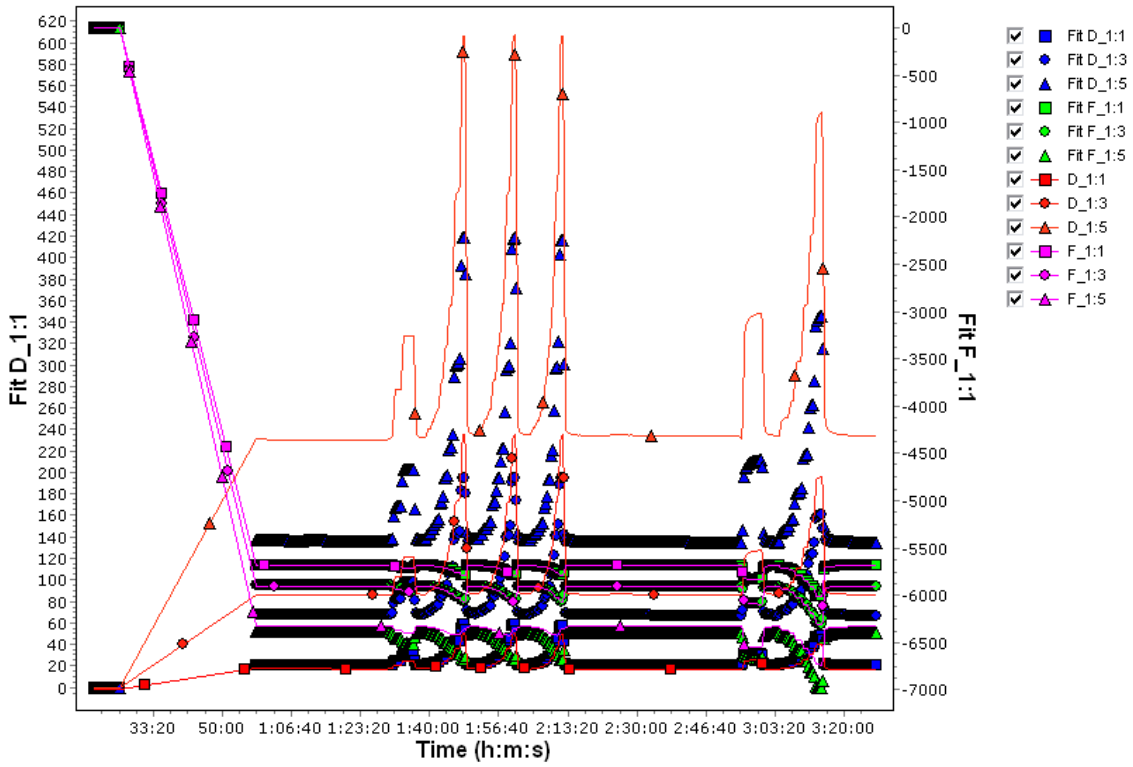

Fig. S18 The experimental and fit values of Δf and ΔD by assuming the film follows the Maxwell viscoelastic model.

a

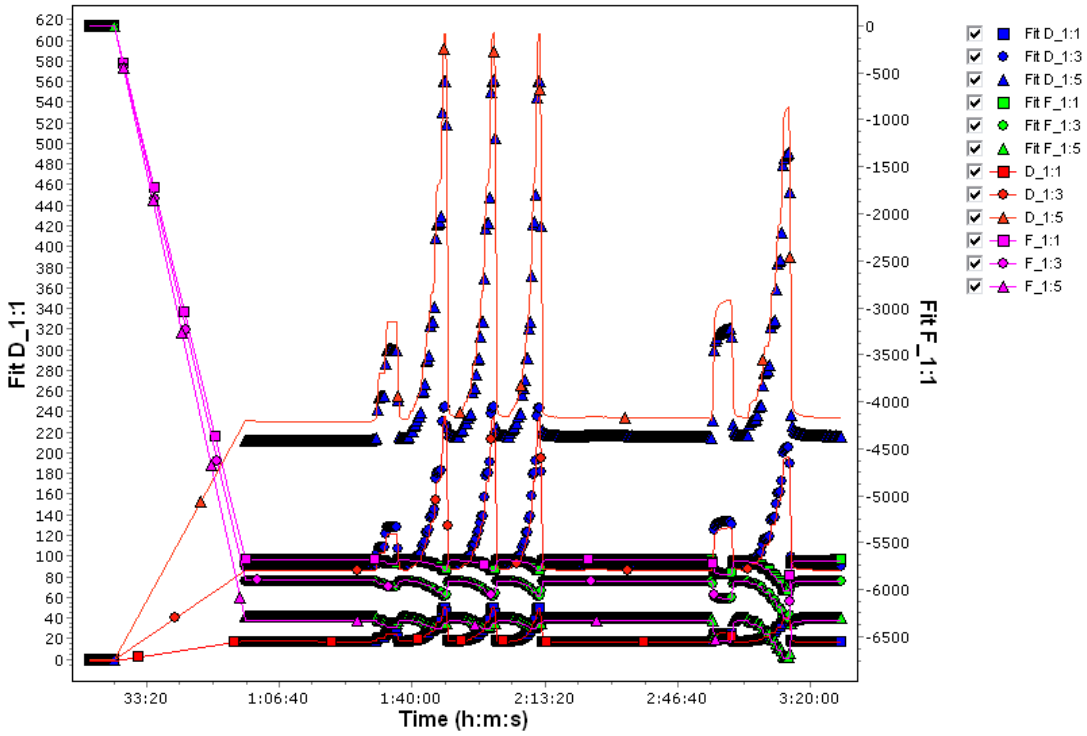
Fit D_1:1
Fit F_1:1
Time (h:m:s)
33:20
1:06:40
1:40:00
2:13:20
2:46:40
3:20:00
Fit D_1:1
Fit D_1:3
Fit D_1:5
Fit F_1:1
Fit F_1:3
Fit F_1:5
D_1:1
D_1:3
D_1:5
F_1:1
F_1:3
F_1:5

b

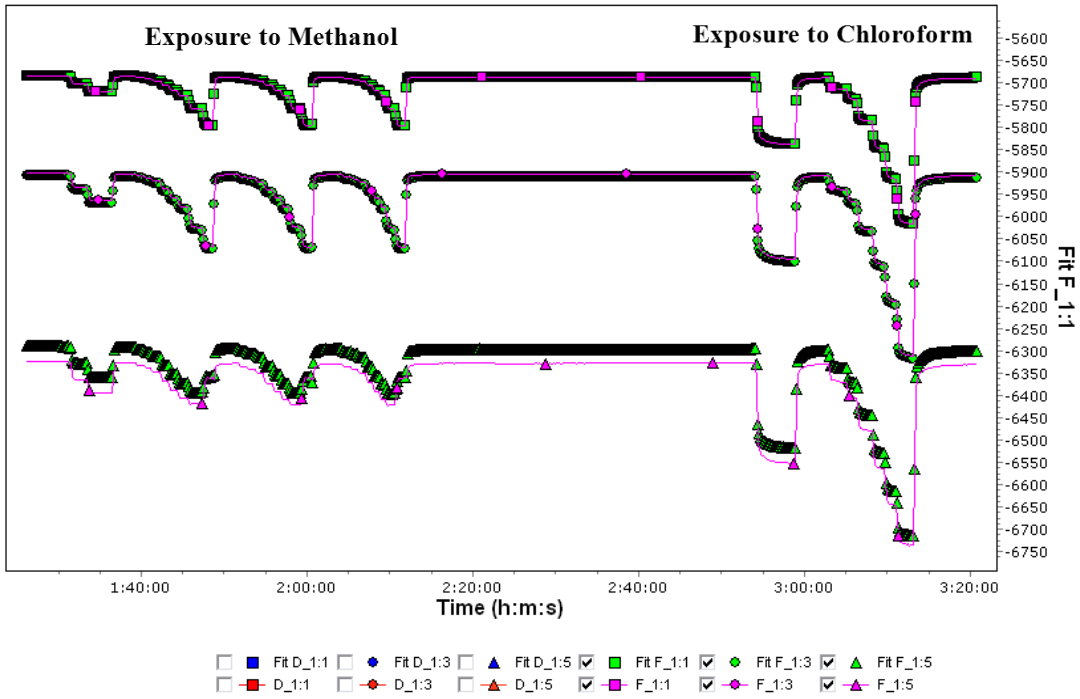
Exposure to Methanol
Exposure to Chloroform
Fit F_1:1
Time (h:m:s)
1:40:00
2:00:00
2:20:00
2:40:00
3:00:00
3:20:00
Fit D_1:1
Fit D_1:3
Fit D_1:5
Fit F_1:1
Fit F_1:3
Fit F_1:5
D_1:1
D_1:3
D_1:5
F_1:1
F_1:3
F_1:5

c

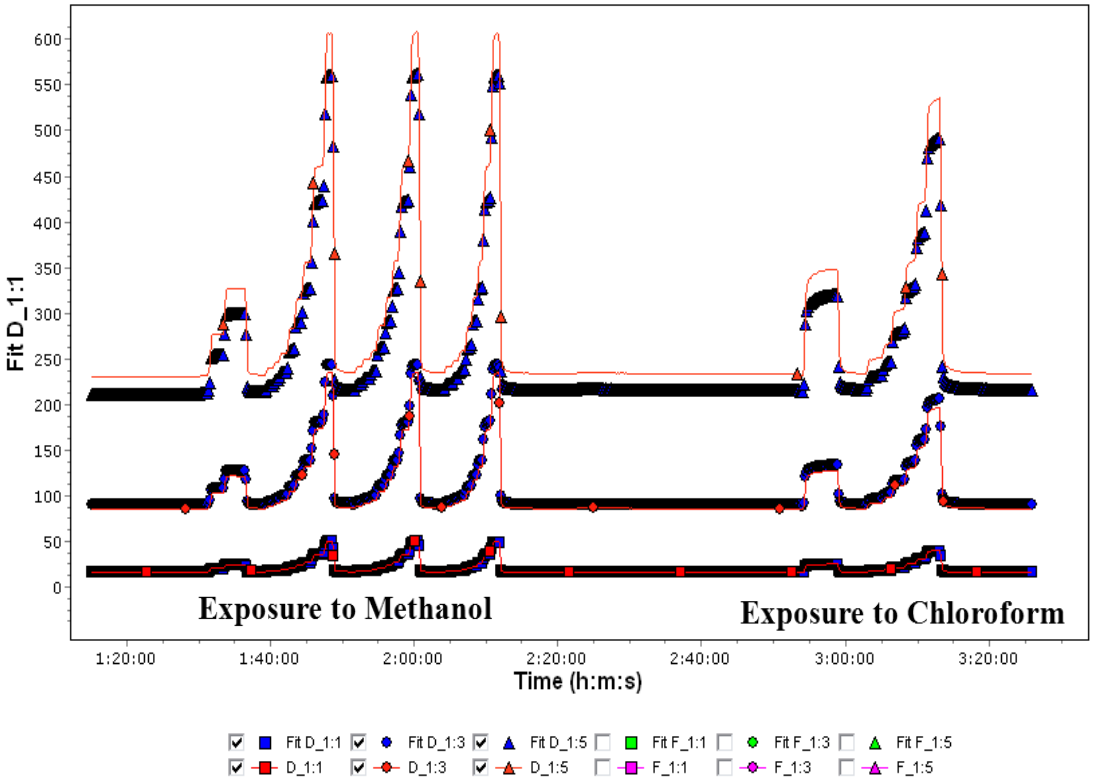

Fig. S19 (a) The experimental and fit values of Δ*f* and Δ*D* using the extended Voigt viscoelastic model, (b) experimental and fit values of Δ*f*, and (c*)* experimental and fit values of Δ*D* shown for clarity.

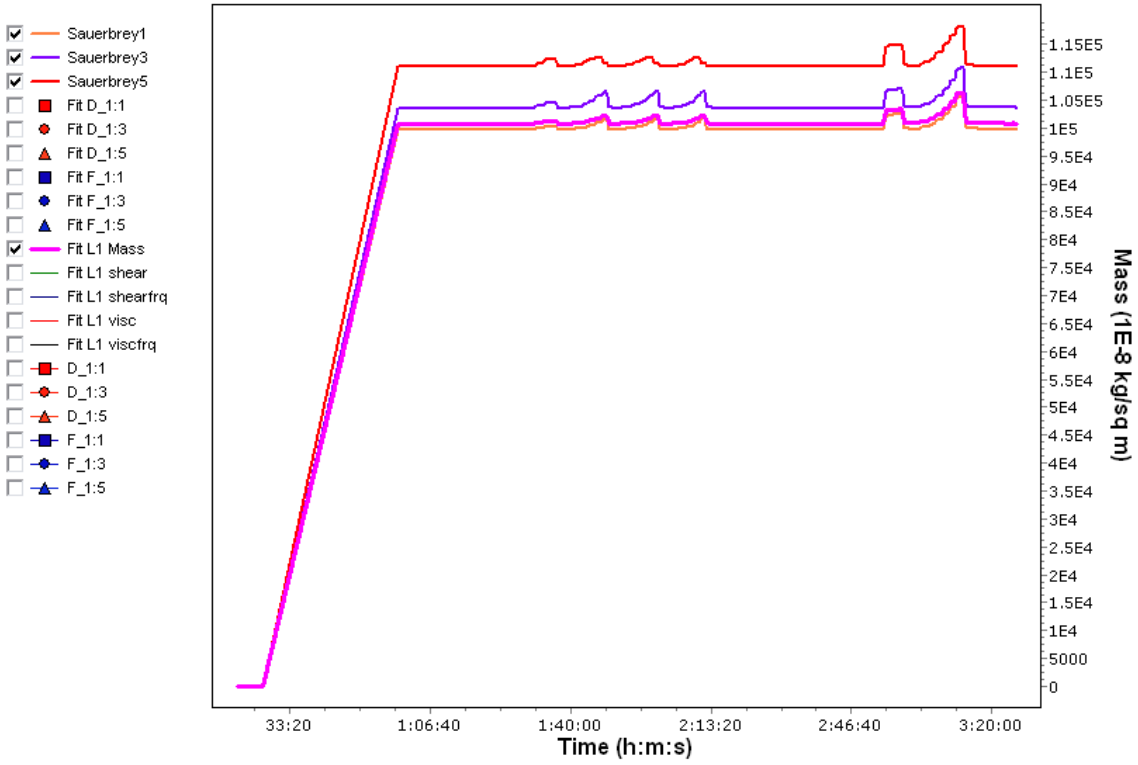

Fig. S20 Mass of the film before and after the uptake of vapors as determined by the Sauerbrey equation at the first, third, and fifth harmonics. The fit mass obtained by using the extended Maxwell viscoelastic model is represented by the bold line.

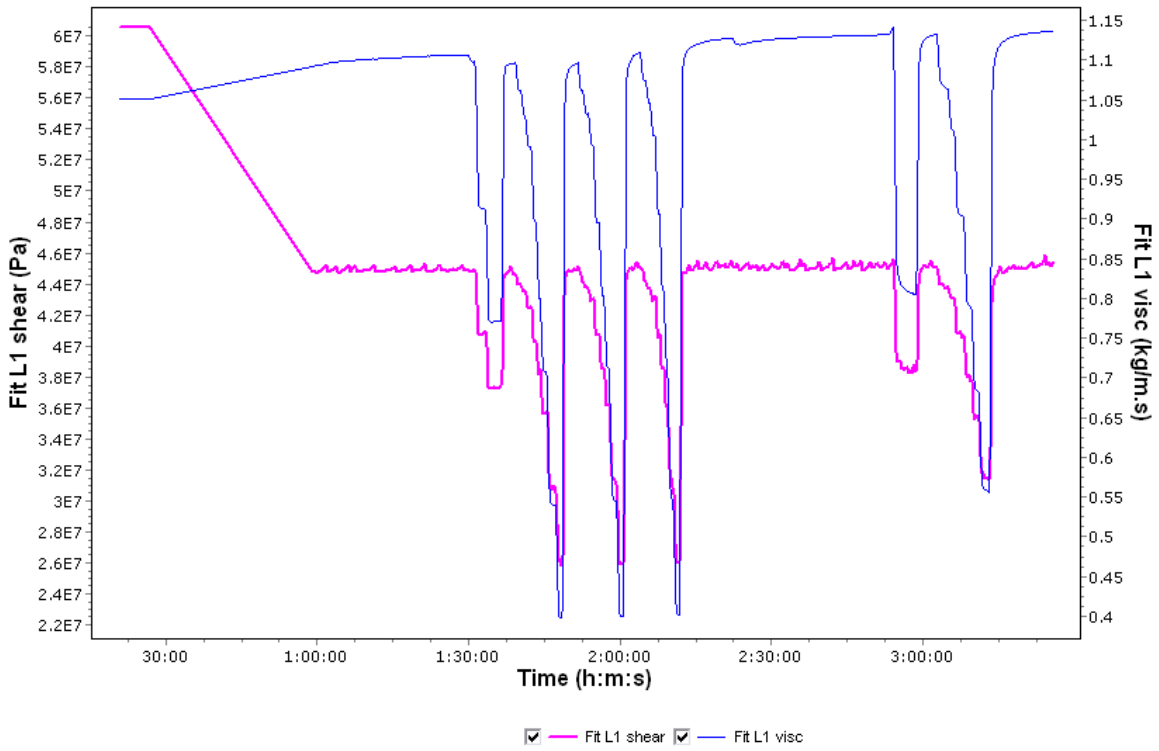

Fig. S21 Changes in elastic shear modulus and viscosity of the film during vapor absorption as predicted by the extended Maxwell viscoelastic model.